

Structural, Morphological, Optical and Dielectric Properties of CuO and SnO₂ Nanoparticles

J. Priya Sharon¹, K. Gnanaprakasam Dhinakar²

¹Research Scholar (Reg. No.: 20212152132002), PG & Research Department of Physics, Pope's College (Autonomous), Sawyerpuram – 628 251, Tamil Nadu, India

²Assistant Professor, PG & Research Department of Physics, Pope's College (Autonomous), Sawyerpuram – 628 251, Tamil Nadu, India

Nanoparticles of copper oxide (CuO) and tin oxide (SnO₂) have been created using a solvothermal process aided by microwaves. The sample was annealed at 450°C for one hour in order to create the CuO and SnO₂ phases. CuO and SnO₂ nanoparticles' crystal structure, shape, and optical band gap were examined using X-ray diffraction (XRD), scanning electron microscopy, UV–visible spectroscopy, and Fourier transform infrared spectroscopy. The annealed CuO and SnO₂ samples displayed a monoclinic and tetragonal crystalline structure with crystallite sizes of around 8 and 12 nm, according to the XRD results. CuO and SnO₂ nanoparticles were found to have optical band gaps of 4.15 eV and 3.86 eV, respectively. CuO and SnO₂ nanoparticles' dielectric characteristics and ac conductivity were examined at various temperatures ranging from 50°C to 175°C.

Keywords: copper oxide; tin dioxide; solvothermal synthesis; nanoparticles; characterization; dielectric study.

1. Introduction

Modern living is made easier by advances in nanoscience and nanotechnologies, which have affected nearly every branch of science. A growing field of study called nanoscience and nanotechnology deals with systems, devices, and structures that have unique characteristics and capabilities because of the way their atoms are arranged on a size of 1–100 nm. Almost all branches of research, including physics, computer science, materials science, chemistry, biology, and engineering, benefit from nanotechnologies ^[1].

An effective wet-chemical method for producing nanomaterials is the microwave-assisted solution route, which also has the benefit of quick volumetric heating, fast reaction rates,

controllable size and shape by reaction parameter adjustment, and energy efficiency [2]. Because the reaction mixture is heated directly, research has demonstrated that this method is an appealing option for promoting reactions and is energy-effective heating when compared to traditional heat conduction methods (like an oil bath) [3].

Based on their structural characteristics, nanoparticles can be simply categorized as zero-, one-, two-, and three-dimensional materials. 0D nanostructured materials (NSMs), like quantum dots, have been thoroughly investigated for use in lasers, solar cells, light-emitting diodes (LEDs), and single-electron transistors. The fields of nanoelectronics, nanodevices and systems, nanocomposite materials, alternative energy resources, and national security are significantly impacted by 1D NSMs. Two-dimensional nanostructured Certain geometries of materials show special shape-dependent properties that lead to their application as fundamental building blocks for nanodevices [4]. Beyond the nanoscale (>100 nm), materials with three arbitrary dimensions are called three-dimensional (3-D) structures. On the other hand, these materials have features at the nanoscale or a nanocrystalline structure [5].

There are various types of nanostructures, including nanocage, nanocrystal, nanobelt, nanofiber, nanoparticle, nanotube, nanorods, nanowire, quantum dots, and nanocomposites [5]. There are two primary classifications for nanoparticle synthesis techniques: top-down and bottom-up approaches. Numerous techniques are available for the chemical synthesis of nanoparticles, such as flow injection, sol-gel, reduction, co-precipitation, nucleation, electrochemical, solvothermal, hydrothermal, and microwave-assisted techniques. The most common physical processes for creating nanoparticles include evaporation-condensation, combustion synthesis, arc discharge/plasma, laser/electron beam heating, and laser ablation technique [6, 7].

Transition metal oxides are substances made up of oxygen atoms attached to transition metals. Their semiconductive qualities and catalytic activity make them widely used. Because of their distinct physical and chemical characteristics, titanium dioxide (TiO_2), cupric oxide (CuO), and zinc oxide (ZnO) have drawn the most interest among the transition metal oxides. Applications for nanoparticles in catalysis, energy storage, water treatment, sensors, nanomedicine, automotive, chemical, food, and cosmetics industries are numerous in the engineering field [8].

This work aims to investigate the impact of several general parameters on the shape and characteristics of CuO and SnO_2 nanomaterials that are generated using a microwave assisted technique.

2. SYNTHESIS METHOD

CuO and SnO_2 nanoparticles were synthesized using a solvothermal process with microwave assistance. Some benefits of using microwave irradiation to synthesize nanoparticles include homogeneous heating of the solutions, a very short processing time, excellent control over particle size, and uniform nucleation of nanocrystals to produce CuO and SnO_2 nanoparticles with a limited size distribution.

2.1. SYNTHESIS OF CuO NANOPARTICLES

The synthesis of CuO nanoparticles involved in three steps

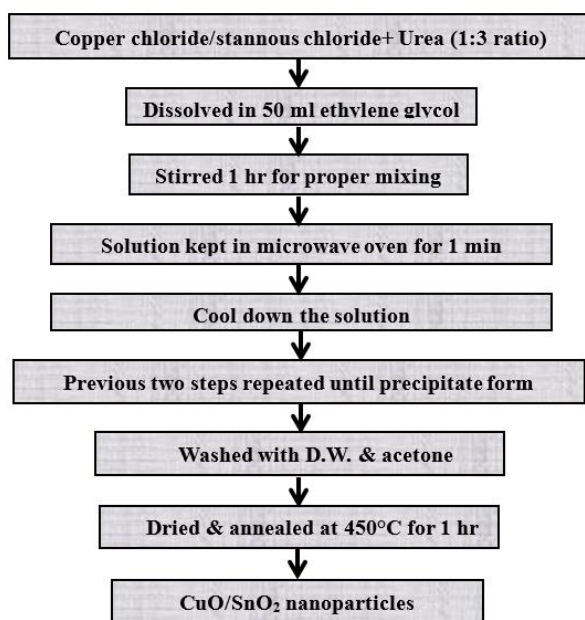
1. Taking the Precursor materials
2. Mixing all the reagents
3. Microwave irradiation and Drying

Analytical Reagent (AR) grade copper chloride, urea as a catalyst, and ethylene glycol as a solvent were the precursors utilized in the production of CuO. In 50 milliliters of ethylene glycol, copper chloride and urea are taken as solutes in a molecular ratio of 1:3, dissolved, and then agitated for an hour using a magnetic stirrer. After being in the microwave for one minute, the resulting solution is cooled. Following cooling, the mixture is once more placed in a microwave oven for a duration of one minute, and this process is repeated until a precipitate is achieved. The resultant precipitate was filtered, cleaned with double-distilled water, and allowed to dry for three days in the sun. The resulting powders underwent two or more acetone washes ^[9]. For the purpose of eliminating any undesired organic materials, the sample was annealed for one hour at 450 degrees Celsius in an air environment. The prepared CuO nanoparticles were green in color before to annealing, but they became black thereafter.

2.2. SYNTHESIS OF SnO₂ NANOPARTICLES

Analytical Reagent (AR) grade stannous chloride, urea as a catalyst, and ethylene glycol as a solvent were the precursors utilized in the manufacture of SnO₂. The SnO₂ nanoparticles were prepared using the same process ^[10]. The produced SnO₂ nanoparticles were white in color; however, annealing caused them to become off-white in color.

2.3. FLOW CHART:



3. Results and Discussion

3.1 STRUCTURAL & MORPHOLOGICAL ANALYSIS

3.1.1 XRD Pattern Results of CuO and SnO₂ Nanoparticles

Figure 3.1 displays the generated copper oxide nanoparticles' XRD spectrum. With a step size of 0.02 s, the XRD data is gathered in a 2θ range covering 10° to 90°. The copper oxide production for which the sample was annealed at 450°C for an hour in order to obtain the copper oxide nanoparticles is confirmed by the XRD data. The major peaks positioned at 2θ values of 32.38°, 35.72°, 38.70°, 49.02°, 53.10°, 61.37°, 65.65°, 67.96°, 75.11° correspond to (110), (002), (111), (202), (020), (202), (113), (311), (113), (311) and (004) crystal planes, respectively ^[11].

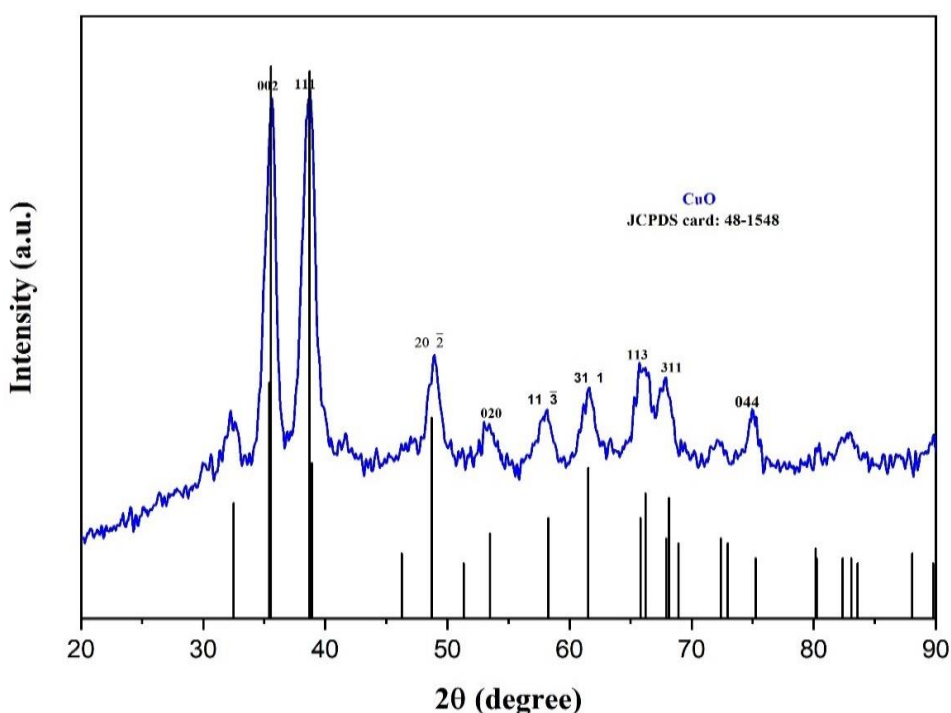


Figure 3.1: XRD spectra of copper oxide nanoparticles

Figure 3.1 shows that the synthesized copper oxide nanoparticles xrd result matched the JCPDS card no.: 48-1548. The lattice parameter is $a=4.688$, $b=3.422$, and $c=5.131$. The observed structure of the copper oxide is monoclinic ^[12]. The creation of pure crystalline CuO by the microwave-assisted approach is shown by the lack of peaks matching to Cu₂O and Cu(OH)₂ in the pattern and the emergence of all peaks belonging to the monoclinic CuO phase ^[13].

The crystallite size of the prepared sample was calculated using the Scherrer equation:

$$D = \frac{K\lambda}{\beta \cos \theta}$$

In this case, β stands for the full width at half maximum (FWHM), $K\alpha$ for the Scherrer's constant (0.9), λ for the X-ray wavelength, and θ for the Bragg's diffraction angle^[10]. CuO nanoparticles computed for the highest peaks at 35.72° and 38.70° had an average crystallite size of around 8 nm^[9].

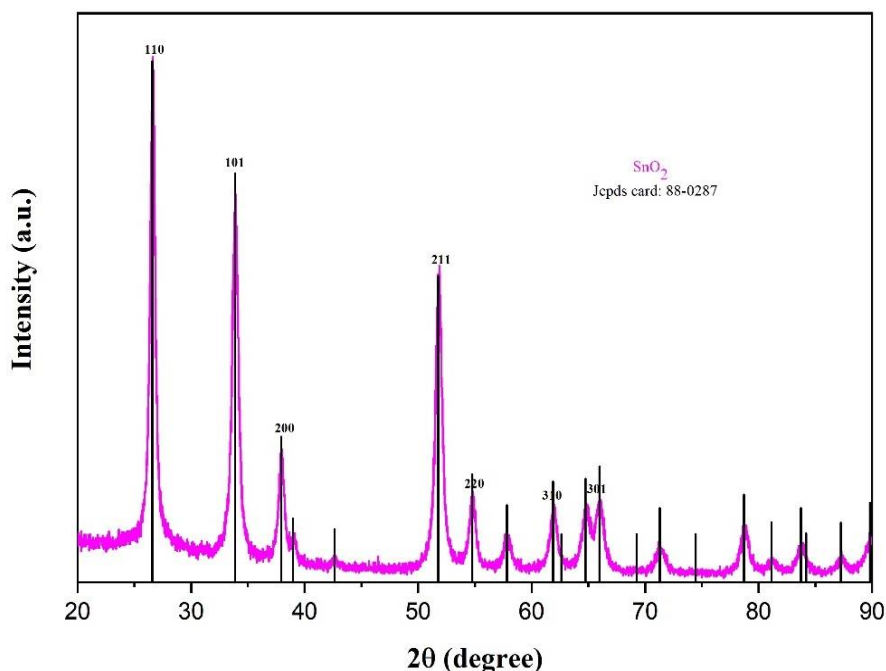


Figure 3.2: XRD spectra of tin oxide nanoparticles

The diffraction peaks of the tin oxide nanoparticles 2θ value are 26.61° , 33.97° , 37.97° , 51.82° , 54.64° , 61.94° , 64.81° , 66.00° , 71.35° and the corresponding hkl plane value are (110), (101), (200), (211), (220), (310), (301)^[14, 15]. Figure 3.2 displays the XRD results for the tin oxide nanoparticles that match the JCPDS card number: 88-0287. $A=4.737$ and $c= 3.186$ are the lattice parameters^[14, 16, 17]. The SnO₂ nanoparticles with the greatest peaks at 26.61° and 33.89° had an average crystallite size of around 12 nm.

3.1.2 SEM Results of CuO and SnO₂ Nanoparticles

Figure 3.3 displays the surface analysis of the SEM image of the sample of copper oxide nanoparticles at various magnifications. The CuO nanostructure produced using a microwave-assisted technique displays an evenly distributed cluster of agglomerated morphology, as seen by the SEM picture^[18]. A high magnification view of figure 3.3 reveals that some particles with spherical morphology are observed apart from the agglomerated clusters^[9, 19].

The XRD results were corroborated by the SEM data. Figure 3.4 shows a SEM picture of the morphology of the tin oxide nanoparticles. The formed tin oxide nanoparticles are synthetic and resemble spheres^[14, 15, 20, 21].

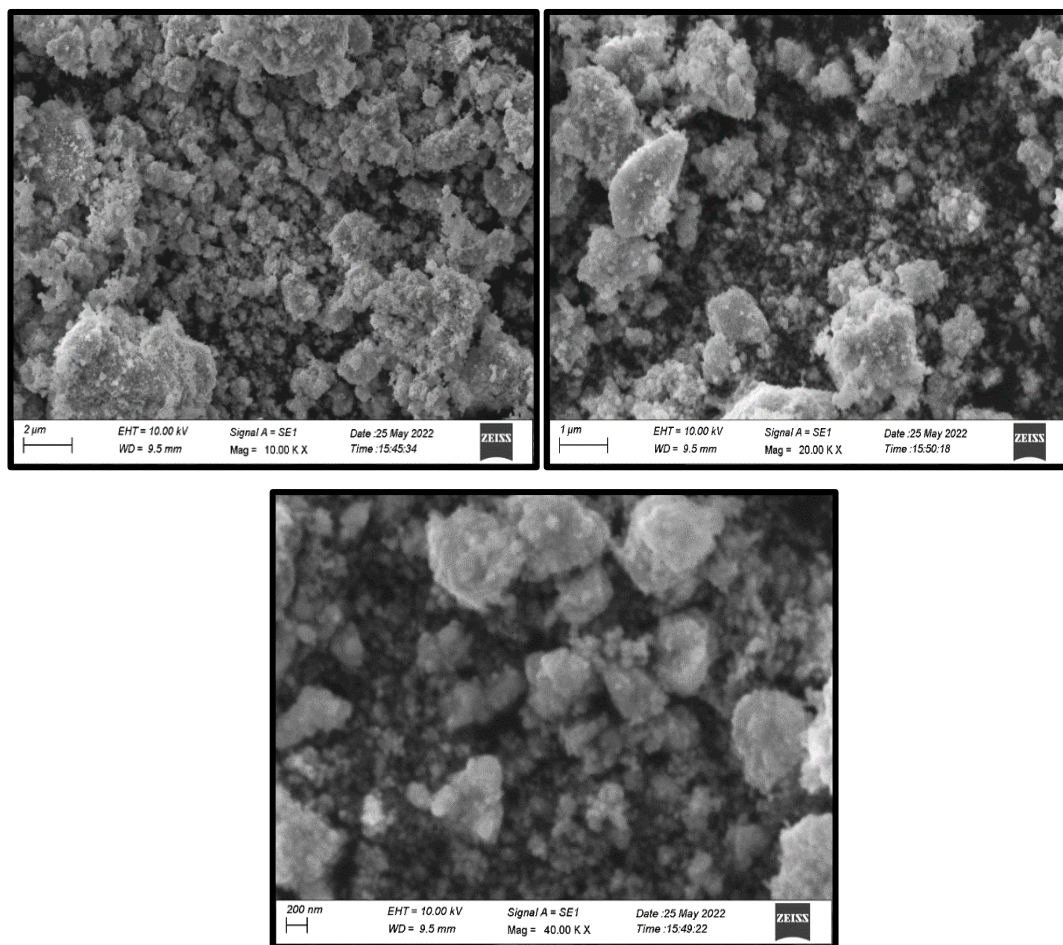


Figure 3.3: SEM image of CuO nanoparticles at different magnification

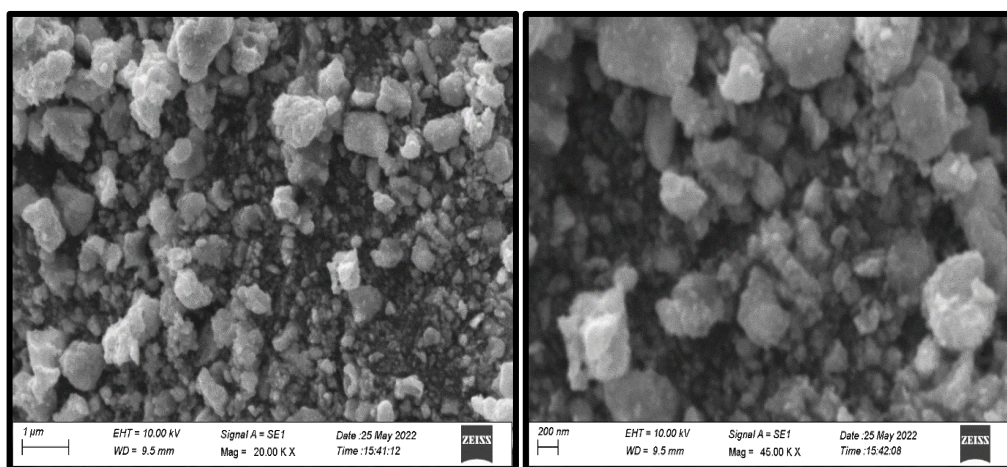


Figure 3.4: SEM image of SnO₂ nanoparticles at different magnification

3.2 FTIR RESULTS OF CuO AND SnO₂ NANOPARTICLES

The range of the FTIR spectrum measured is 4000–400 cm^{-1} . The bands at 3133 cm^{-1} in figure 3.5 match the vibrational frequency stretching of the O-H functional groups^[12]. The stretching vibrations of the C=C aromatic ring are represented by the bands at 1654 cm^{-1} ^[9]. The C-H out of smooth deformation is responsible for the bands that emerged at 1400 cm^{-1} ^[19]. The range below 1000 cm^{-1} is often where the bands resulting from the metal-oxygen (M-O) bond's vibrational frequencies occur^[9]. Therefore, the peaks at 477 and 532 cm^{-1} are indicative of the distinctive Cu-O bond vibration that reveals the creation of CuO nanoparticles^[10, 12].

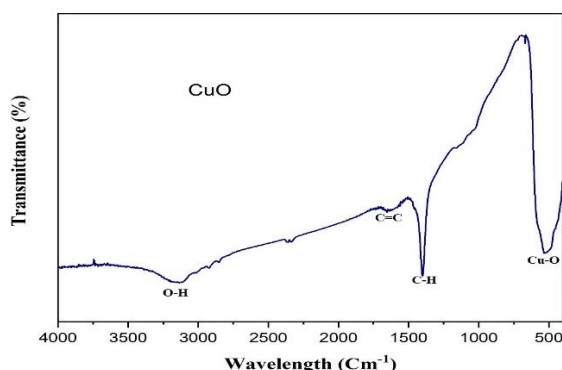


Figure 3.5: FTIR spectra of CuO nanoparticles

The SnO₂ sample's FTIR spectra are displayed in Figure 3.6. The O-H functional group is represented by the band that occurred at 3130 cm^{-1} . The 700–400 cm^{-1} region is where the main infrared peaks for the Sn–O and O–Sn–O bond vibrations are found^[22]. The strong peak observed at 620 cm^{-1} can be assigned to Sn–O–Sn^[20]. The carbonyl group of the carboxylate ions, which may stay absorbed on the surface, is connected to the peak at 1400 cm^{-1} .

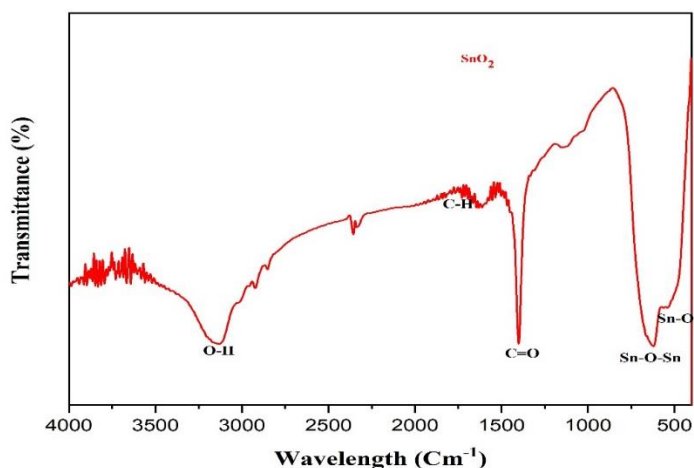


Figure 3.6: FTIR spectra of SnO₂ nanoparticles

3.3 UV-VIS RESULTS OF CuO AND SnO₂ NANOPARTICLES

A potent non-destructive testing technique for examining the optical characteristics of semiconductor nanoparticles is absorption spectroscopy. Certain characteristics, such as the band gap, oxygen deficit, surface type, and impurity centers, may affect the absorbance. The absorbance spectrum of copper oxide nanoparticles peaks at 278 nm, as seen in Figure 3.7^[12, 23].

The relation between incident photon energy and absorption coefficient can be defined as

$$(\alpha h\nu)^{1/n} = A (h\nu - E_g)$$

Where A is the constant, E_g is the band gap of the material and n is the exponent depend on the type of the transition ^[10, 11, 21]. The band gap energy value is 4.15 eV calculated by tauc's plot ^[24].

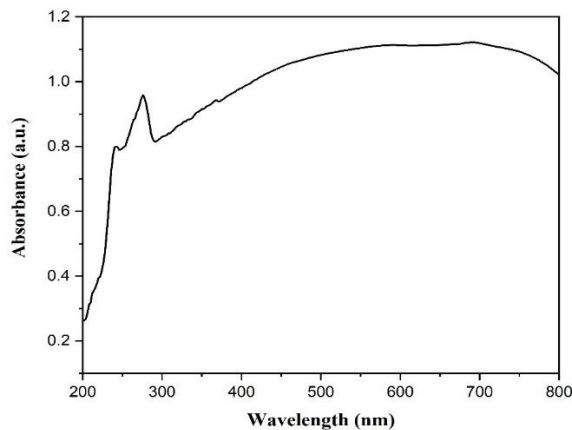


Figure 3.7: UV-Visible spectrum of CuO nanoparticles

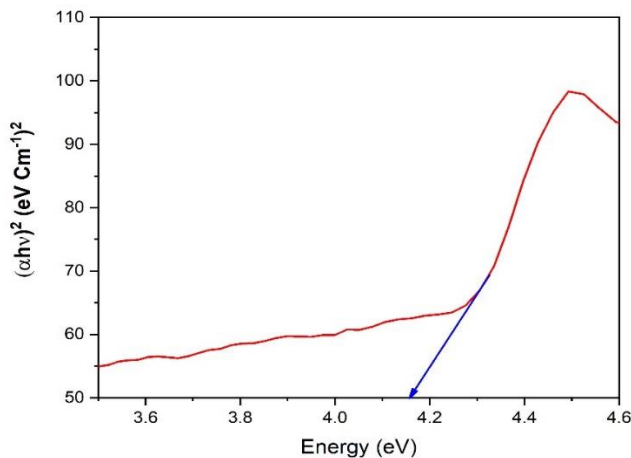
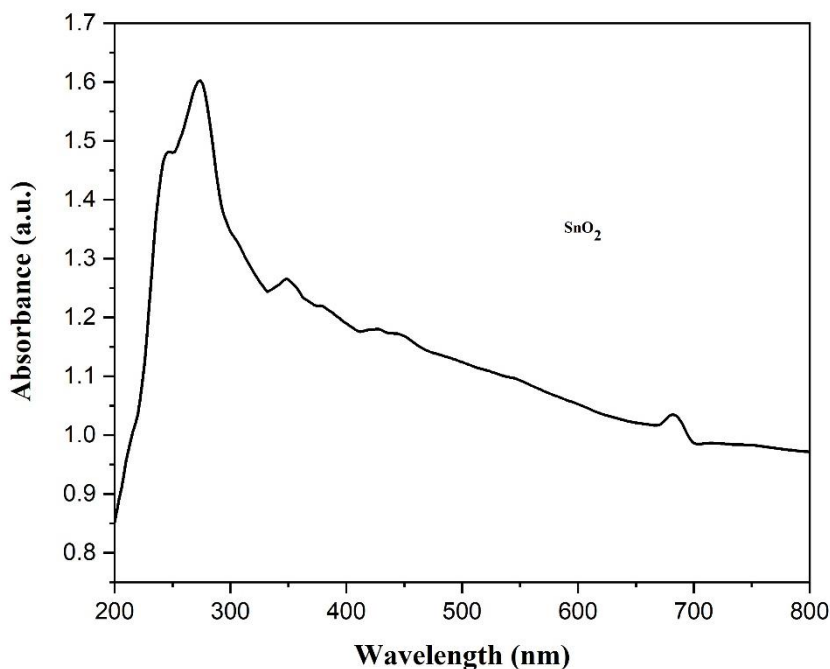
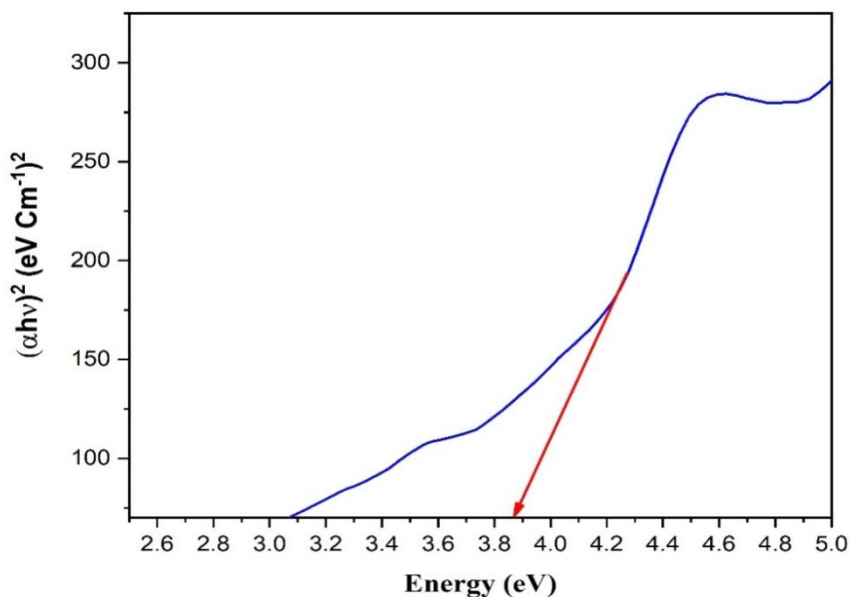


Figure 3.8:Tauc's plot of CuO nanoparticles

Figure 3.9: UV-Visible spectrum of SnO₂ nanoparticlesFigure 3.10: Tauc's plot of SnO₂ nanoparticles

The 200–800 nm range is covered by the UV–visible spectrum ^[14]. In close accord with previous results, the UV-visible absorption spectra of tin oxide nanoparticles exhibit peaks around 273 nm, which are attributable to the production of tin oxide nanoparticles. 3.86 eV is the estimated band gap energy ^[17, 21].

3.4 DIELECTRIC STUDY:

The formula for calculating the Dielectric constant^[22] was

$$\epsilon' = ct/(\epsilon_0 A)$$

An electrical conductivity (σ_{ac}) was evaluated according to the relation:

$$\sigma_{ac} = 1/\rho$$

$$\rho = \frac{A}{2\pi fct}$$

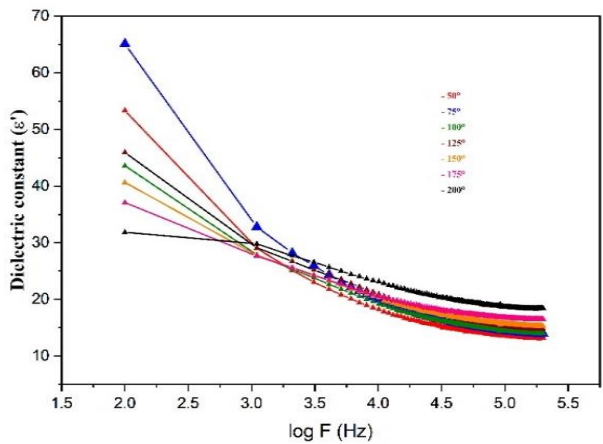


Figure 3.11: Frequency vs dielectric constant for CuO nanoparticles

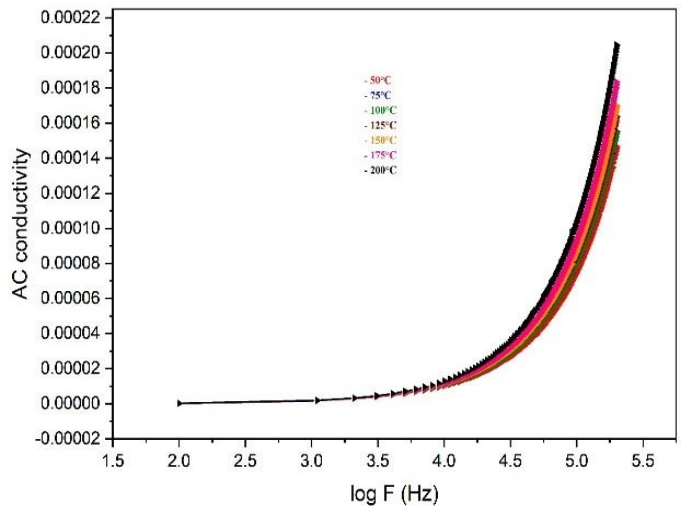


Figure 3.12: Frequency vs ac conductivity for CuO nanoparticles

Figures 3.11, 3.12, 3.13, and 3.14 illustrate how the synthesized copper oxide (CuO) and tin oxide (SnO₂) had a decreasing dielectric constant and an increasing ac conductivity as the temperature increased from 50°C to 175°C. The dielectric constant (ϵ') is reported to exhibit dispersion at lower frequencies, decreasing sharply and reaching saturation for higher frequencies^[22]. The dielectric constant changes as a function of applied frequency because of charge transport relaxation time. The interfacial polarization is responsible for this dielectric dispersion^[15]. The conduction mechanism and the type of polarons responsible for conduction, the variation of ac conductivity as a function of frequency.

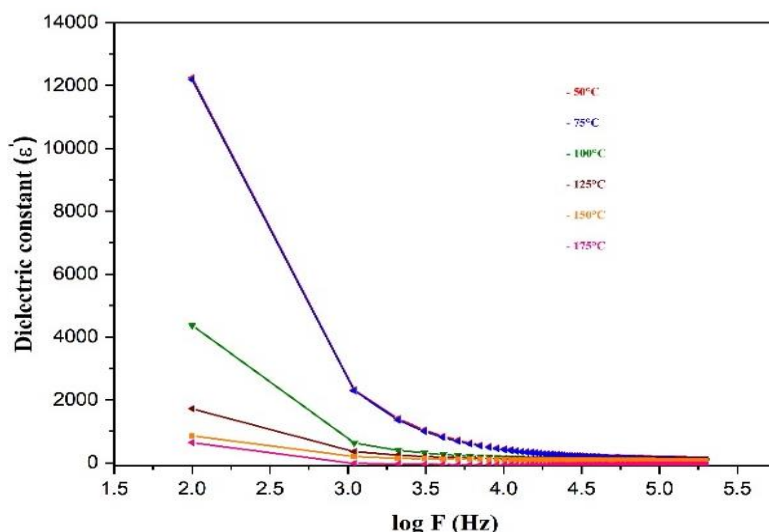


Figure 3.13: Frequency vs dielectric constant for SnO₂ nanoparticles

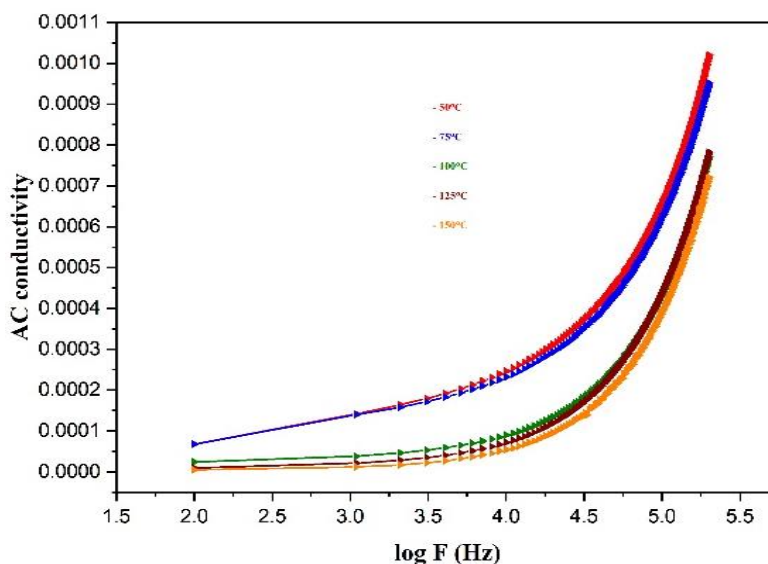


Figure 3.14: Frequency vs ac conductivity for SnO₂ nanoparticles

4. Conclusion

Applications for nanoparticles are widespread across the world. Particle characteristics alter transversely as size decreases, and these changes are beneficial in a variety of applications. This work uses a microwave-assisted technique to manufacture the tin oxide and copper oxide nanoparticles. The synthesized nanoparticles were examined using a variety of tools, including dielectric studies, FTIR, UV-visible, SEM, and XRD. The average crystallite size was also determined using the XRD spectra, which further validates the creation of copper oxide and tin oxide nanoparticles. To identify the functional groups, the FTIR spectra of the copper oxide and tin oxide samples were recorded.

The X-ray diffraction results corroborate the scanning electron microscopy results of CuO and SnO₂ nanoparticles. SEM images showed the copper oxide and tin oxide nanoparticles shape. The peaks at 477 and 532 cm⁻¹ are part of the distinctive Cu-O bond vibration that indicates the production of CuO nanoparticles. Sn-O-Sn can be attributed to the prominent peak that was detected at 620 cm⁻¹. The materials' UV-visible absorbance spectra were measured between 200 and 800 nm. Using Tauc's figure, the energy band gap values for copper oxide and tin oxide nanoparticles were determined to be 4.15 eV and 3.86 eV respectively. As the temperature rose from 50°C to 175°C, the artificial copper oxide (CuO) and tin oxide (SnO₂) showed a falling dielectric constant and an increasing ac conductivity. According to reports, the dielectric constant (ϵ') exhibits dispersion at lower frequencies before drastically falling and achieving saturation at higher frequencies.

References

1. Bayda, S., Adeel, M., Tuccinardi, T., Cordani, M., & Rizzolio, F. (2019). The history of nanoscience and nanotechnology: from chemical–physical applications to nanomedicine. *Molecules*, 25(1), 112. DOI: 10.3390/molecules25010112.
2. Saleh, T. A., Majeed, S., Nayak, A., & Bhushan, B. (2017). Principles and advantages of microwave-assisted methods for the synthesis of nanomaterials for water purification. In *Advanced nanomaterials for water engineering, treatment, and hydraulics* (pp. 40-57). IGI Global. DOI: 10.4018/978-1-5225-2136-5.ch003.
3. Motshekga, S. C., Pillai, S. K., Sinha Ray, S., Jalama, K., & Krause, R. (2012). Recent trends in the microwave-assisted synthesis of metal oxide nanoparticles supported on carbon nanotubes and their applications. *Journal of Nanomaterials*, 2012. DOI: 10.1155/2012/691503.
4. Tiwari, J.N., Tiwari, R.N., & Kim, K.S. (2012). Zero-dimensional, one-dimensional, two-dimensional and three-dimensional nanostructured materials for advanced electrochemical energy devices. *Progress in Materials Science*, 57(4), 724-803. DOI: 10.1016/j.pmatsci.2011.08.003.
5. Saleh, T.A., & Gupta, V.K. (2016). Synthesis, classification, and properties of nanomaterials. *Nanomaterial and Polymer Membranes*. Elsevier, 2016, 83–133. DOI:10.1016/b978-0-12-804703-3.00004-8.
6. Ijaz, I., Gilani, E., Nazir, A., & Bukhari, A. (2020). Detail review on chemical, physical and green synthesis, classification, characterizations and applications of nanoparticles. *Green Chemistry Letters and Reviews*, 13(3), 223-245. DOI: 10.1080/17518253.2020.1802517.
7. Mageswari, A., Srinivasan, R., Subramanian, P., Ramesh, N., & Gothandam, K. M. (2016). Nanomaterials: classification, biological synthesis and characterization. In *Nanoscience in Food and Agriculture 3* (pp. 31-71). Springer, Cham. DOI: 10.1007/978-3-319-48009-1_2.
8. Bratovcic, A. (2019). Different applications of nanomaterials and their impact on the *Nanotechnology Perceptions* Vol. 20 No.7 (2024)

- environment. *International Journal of Material Science and Engineering*, 5(1), 1-7.
9. Vallimeena, S., et al. "Structural and optical properties of pure and cobalt doped tin oxide nanoparticles."
 10. Bekru, AkliluGuale, et al. "Microwave-assisted synthesis of CuO nanoparticles using cordiaafricana Lam. leaf extract for 4-nitrophenol reduction." *Journal of Nanotechnology* 2021 (2021).
 11. Felix, S., R. Bala Praveen Chakkravarthy, and A. Nirmala Grace. "Microwave assisted synthesis of copper oxide and its application in electrochemical sensing." *IOP Conference Series: Materials Science and Engineering*. Vol.73. No.1.IOP Publishing, 2015.
 12. Sutradhar, Prasanta, MitaliSaha, and DebasishMaiti. "Microwave synthesis of copper oxide nanoparticles using tea leaf and coffee powder extracts and its antibacterial activity." *Journal of Nanostructure in Chemistry* 4.1 (2014): 1-6.
 13. Okpara, Enyioma C., et al. "Green synthesis of copper oxide nanoparticles using extracts of Solanummacrocarpon fruit and their redox responses on SPAu electrode." *Heliyon* 7.12 (2021): e08571.
 14. Krishnakumar, T., et al. "Synthesis and characterization of tin oxide nanoparticle for humidity sensor applications." *Journal of Nano Research*. Vol. 4. Trans Tech Publications Ltd, 2008.
 15. Babar, A.R., et al. "Electrical and dielectric properties of co-precipitated nanocrystallinetin oxide." *Journal of Alloys and Compounds* 505.2 (2010): 743-749.
 16. Gnanam, S., and V. Rajendran. "Synthesis of tin oxide nanoparticles by sol–gel process: effect of solvents on the optical properties." *Journal of sol-gel science and technology* 53.3 (2010): 555-559.
 17. He, Zuoli, and Jiaqi Zhou. "Synthesis, characterization, and activity of tin oxide nanoparticles: influence of solvothermal time on photocatalytic degradation of rhodamine B." *Mod. Res. Catal* 2 (2013): 13-18.
 18. Vijayashree, K., K. Sheshappa Rai, and T. Demappa. "Synthesis of nanosized copper oxide by assimilating microwave radiation and its characterizations." *Indian Journal of Advances in Chemical Science* S1 6 (2016): 9.
 19. Quirino, Max Rocha, et al. "CuO rapid synthesis with different morphologies by the microwave hydrothermal method." *Materials Research* 21 (2018).
 20. Chand, Prakash, Anurag Gaur, and Ashavani Kumar. "Study of CuO nanoparticles synthesized by sol-gel method." *AIP Conference Proceedings*. Vol. 1393. No. 1. American Institute of Physics, 2011.
 21. Bhagwat, Ashok D., et al. "Synthesis of nanostructured tin oxide (SnO₂) powders and thin films prepared by sol-gel method." (2015).
 22. Balakrishnan, Kavitha, and Nirmala Murugasean. "Synthesis and characterization of SnO₂ nanoparticles by co-precipitation method." *International Journal of Nano Dimension* 12.1 (2021): 76-82.
 23. Wang, Hui, et al. "Preparation of CuO nanoparticles by microwave irradiation." *Journal of crystal growth* 244.1 (2002): 88-94.
 24. Jayakodi, Santhoshkumar, and Venkat Kumar Shanmugam. "Green synthesis of CuO nanoparticles and its application on toxicology evaluation." *Biointerface Res. Appl. Chem* 10 (2020): 6343-6353.